

Quantum proton transfer with spatially dependent friction: Phenol-amine in methyl chloride

Dimitri Antoniou and Steven D. Schwartz

Department of Physiology and Biophysics, Albert Einstein College of Medicine, 1300 Morris Park Avenue, Bronx, New York 10461

(Received 24 November 1998; accepted 22 January 1999)

In a recent paper [D. Antoniou and S. D. Schwartz, *J. Chem. Phys.* **110**, 465 (1999)] we calculated the reaction rate for a proton transfer reaction in liquid methyl chloride. In that work, we used a spectral density obtained from a molecular dynamics simulation as input to a quantum Zwanzig Hamiltonian which we solved using our exponential resummation method. In the present paper we perform a similar calculation, allowing for a position dependent friction using the method of G. Haynes, G. Voth, and E. Pollak [*J. Chem. Phys.* **101**, 7811 (1994)]. Compared with the results of our previous work, we found that including spatial dependence to the friction led to enhancement of the reaction rate and to reduction of the *H/D* kinetic isotope effect. © 1999 American Institute of Physics. [S0021-9606(99)51715-7]

I. INTRODUCTION

In the last few years substantial progress has been made in the study of quantum reaction rates in solution. Most of these studies model the coupling of the reaction coordinate to the environment through a spectral density. The advantage of this approach is that one can start from some realistic intermolecular potentials and perform a molecular dynamics (MD) simulation in order to calculate a spectral density, which can then be used in a rate calculation. In a previous paper¹ we applied this methodology to a quantum study of proton transfer in liquid methyl chloride. A limitation of this approach is an implicit assumption that the friction is independent of the position of the reaction coordinate. In the present paper we have repeated our quantum calculation of the methyl chloride system, this time including a position dependent friction. In order to explain the methodology we have followed, we will first discuss some concepts and results from classical rate theory.

A large number of activated barrier crossing reactions in liquids can be adequately described by the generalized Langevin equation (GLE)

$$m_s \ddot{s} = -\frac{\partial V(s)}{\partial s} + \int_0^t dt' \gamma(t-t') \dot{s} + F(t), \quad (1.1)$$

where $V(s)$ is the potential along the reaction coordinate s , $F(t)$ is the fluctuating force of the environment, and $\gamma(t)$ is the dynamical friction which obeys the fluctuation-dissipation theorem²

$$\gamma(t) = \frac{1}{k_B T} \langle F(0) e^{-i\hat{Q}\hat{L}t} F(0) \rangle. \quad (1.2)$$

Here, \hat{L} is the Liouville operator and the operator \hat{Q} projects² onto the orthogonal complement of \dot{s} . There are good arguments^{3,4} that suggest that a reasonable way to calculate

$e^{-i\hat{Q}\hat{L}t} F(0)$ is the “clamping” approximation where the force $F(t)$ is calculated while holding the reaction coordinate fixed at the top of the barrier.

It has been established experimentally that the GLE is a good description for a large number of systems. A critical assumption in Eq. (1.1) is that the friction kernel $\gamma(t)$ is independent of the position s . However, it is now known from numerical simulations⁵ that for some reactions in solution this assumption is violated. Before we show how we can incorporate a spatially dependent friction in the framework of the GLE (and later, in a quantum activation rate calculation), we need to recall three important results from the theory of reaction rates.

The first result is the Kramers–Grote–Hynes theory.⁶ Kramers⁷ assumed Markovian dynamics and solved the Fokker–Plank equation in two limiting cases, for high and low friction. Further progress along this direction was made by Grote and Hynes^{3,8} who included memory effects in their Langevin equation study which they solved in the high-friction limit. They found a transfer rate equal to the transition state theory (TST) rate, times the Grote–Hynes coefficient $\kappa_{GH} = \lambda_0^\ddagger / \omega_b$, where λ_0^\ddagger is the frequency of the unstable mode³ at the transition state and ω_b is the inverted barrier frequency.

The second result, which provided a microscopic foundation to the Langevin equation, was the proof⁹ by Zwanzig that when the dynamics of a system obeying the classical Hamiltonian

$$H = \frac{P_s^2}{2m_s} + V(s) + \sum_k \left[\frac{P_k^2}{2m_k} + \frac{1}{2} m_k \omega_k^2 \left(q_k - \frac{c_k s}{m_k \omega_k^2} \right)^2 \right], \quad (1.3)$$

is integrated in the bath coordinates, the generalized Langevin equation [Eq. (1.1)] is obtained if one is willing to pass to the continuum limit. The coupling of the reaction coordinate to the environment is expressed through the terms $c_k s q_k$ in Eq. (1.3). The GLE viewpoint requires knowledge of the

dynamical friction $\gamma(t)$, which can be expressed in terms of the microscopic coefficients c_k, m_k, ω_k that appear in Eq. (1.3) as

$$\gamma(t) = \sum_k \frac{c_k^2}{m_k \omega_k^2} \cos(\omega_k t), \quad (1.4)$$

for a discrete bath. It is important to notice that the solution of the GLE depends only on $\gamma(t)$ and not on the particular set of parameters c_k, m_k, ω_k that generate it through Eq. (1.4). We shall see in Sec. II that the GLE can be generalized for a spatially dependent friction by changing the form of the coupling $c_k s q_k$ in Eq. (1.3) [see Eq. (2.1) below].

The third result was the establishment of a connection between the TST and GLE viewpoints by Pollak.¹⁰ He first solved for the normal modes of the Hamiltonian Eq. (1.3) and then used the result in a calculation of the reaction rate through the multidimensional transition state theory. Somewhat unexpectedly, he rederived the Kramers–Grote–Hynes result. In order to make this result more intelligible we should point out that the modes k in Eq. (1.3) need not (except in the crystalline case) refer to actual modes of the system; rather, they represent a hypothetical environment¹¹ that generates a dynamical friction $\gamma(t)$ through Eq. (1.4), such that when entered in the GLE Eq. (1.1) provides an accurate description of the dynamics. This means that the Grote–Hynes theory is a *transition state theory for this hypothetical environment*.

These results solidified our understanding of rates of reaction in solution and led naturally to a scheme for rate calculations that has been employed often⁴ and uses as input a molecular dynamics simulation:

(i) Perform a molecular dynamics simulation and calculate the force–force correlation function, which according to Eq. (1.2) is proportional to the dynamical friction $\gamma(t)$.

(ii) Solve the Kramers problem that corresponds to a dynamical friction equal to the one calculated in step (i). Then the Kramers–Grote–Hynes correction to the TST rate is obtained.

Moreover, this scheme has also been used in quantum calculations, for example in the investigations cited in Ref. 12 and in our previous quantum calculation¹ for the system we examine in this paper. The reasoning behind using a molecular dynamics simulation as input to a quantum calculation is that since most of the solvent modes are of low frequency, they are thermally excited and it is justifiable to use classical dynamics to calculate the spectral density Eq. (3.1). Then one can solve a quantum generalization of the Zwanzig Hamiltonian Eq. (1.3); the bath oscillators are considered to be quantum mechanical instead of classical (we shall discuss later the validity of this assumption). We should emphasize that there is not any oversimplification involved in treating the bath as harmonic, since, in the framework of the generalized Langevin equation, the only observable is the friction $\gamma(t)$ of Eq. (1.4); therefore we can use in the Zwanzig Hamiltonian Eq. (1.3) any harmonic bath that reproduces the correct friction kernel $\gamma(t)$. It is the case, however, that the GLE/Kramers–Grote–Hynes/Pollak approach is still an approximate one. One approximation, as mentioned above, is the independence of friction on the reaction coordinate posi-

tion. The goal of the work presented in this paper is to show how important this approximation is in a real chemical system and how the assumption can be relaxed and the result corrected.

The structure of this paper is as follows. In the next section we will show how the GLE can be generalized to include position-dependent friction. In Sec. III we will apply this method to a quantum calculation of proton transfer in chloromethane. We have studied this system in an earlier work¹ assuming position-independent friction. Our new calculations will show that the position dependent friction does significantly affect both the reaction rate and the kinetic isotope effect.

II. SPATIALLY DEPENDENT FRICTION

A lot of attention has focused recently on the problem of Langevin equation with spatially dependent friction.^{13–19} There have been two approaches to the problem.

The first¹⁷ is a variational approach that maps the position-dependent problem to an effective parabolic barrier transfer problem, with an effective friction that is position-independent. This approach leads to a result for the rate that can be interpreted as a Grote–Hynes coefficient with a position-dependent friction.

The second approach¹⁸ starts from the modified Langevin Eq. (2.2) and uses the equivalence of the Kramers theory to the multidimensional TST. It has been established^{16,18} by numerical comparison that there is agreement between the two approaches.

In this work we shall follow the Langevin equation approach. In the spirit of Zwanzig's work we start from the following Hamiltonian:

$$H = \frac{P_s^2}{2m_s} + V(s) + \sum_k \left[\frac{P_k^2}{2m_k} + \frac{1}{2} m_k \omega_k^2 \left(q_k - \frac{c_k g(s)}{m_k \omega_k^2} \right)^2 \right]. \quad (2.1)$$

The position dependent part of the friction is manifest in the spatial dependence of the coupling function $g(s)$. The bilinear coupling case is recovered when $g(s) = s$. An assumption has been made that the functional form of the coupling $g(s)$ is the same for all modes k .

Carmeli and Nitzan have shown¹³ that the dynamics of the Hamiltonian Eq. (2.1) is equivalent to that of the effective Langevin equation

$$m_s \ddot{s} = - \frac{\partial V}{\partial s} + \int_0^t dt' \frac{dg[s(t)]}{ds} \frac{dg[s(t')]}{ds} \gamma(t-t') \dot{s} + \frac{dg[s(t)]}{ds} F(t), \quad (2.2)$$

where $F(t)$ is the random force when the reaction coordinate is clamped on the transition state. Equation (2.2) shows that the effective friction kernel is not only nonlocal in time, but also depends on a time-correlated product of derivatives of the coupling function. As we mentioned in the introduction, the molecular dynamics simulations of the GLE are performed by clamping the reaction coordinate on some posi-

tion along the reaction path. In that case, dg/ds is independent of time and Eq. (2.2) has the form of a GLE with random force

$$\frac{dg}{ds}F(t), \quad (2.3)$$

and a friction kernel that satisfies the following fluctuation–dissipation theorem:

$$\gamma_s(t) = \frac{1}{k_B T} \left(\frac{dg}{ds} \right)^2 \langle F(t)F(0) \rangle_{s^\ddagger}, \quad (2.4)$$

where the subscript s^\ddagger means that the average is taken with the reaction coordinate clamped on the transition state.

It is convenient to introduce a new function

$$G(s) \equiv \left(\frac{dg}{ds} \right)^2, \quad (2.5)$$

whose physical meaning will be clear shortly. $G(s)$ obeys the boundary condition

$$\lim_{s \rightarrow s^\ddagger} G(s) = 1. \quad (2.6)$$

The bilinear coupling case (i.e., position-independent friction) corresponds to $G(s) = 1$, or equivalently, to $\gamma_{s=s^\ddagger}$. The position-dependent friction Eq. (2.4) can then be written as

$$\gamma_s(t) = \left(\frac{dg}{ds} \right)^2 \gamma_{s^\ddagger}(t) = G(s) \gamma_{s^\ddagger}(t), \quad (2.7)$$

which shows that $G(s)$ is the reaction coordinate-dependent part of the friction.

We should point out that Eq. (2.7) indicates that the function $G(s)$ can be obtained from the value of the friction kernel at $t=0$. This is a consequence of the fact that the friction kernel is calculated in the clamping approximation. In any case, Eq. (2.7) allows for the calculation of $G(s)$ without the numerical difficulties that plague the long-time tail of molecular dynamics simulations.

One can invert Eq. (2.5) and write

$$g(s) = \int_{s^\ddagger}^s ds' \sqrt{G(s')}. \quad (2.8)$$

Of course, the function $G(s)$ does not contain any new information in addition to $g(s)$. The reason that two physically equivalent quantities have been introduced is that there are two approaches to the dynamics of charge transfer, as explained in the introduction: either one starts from the GLE [when $\gamma_s(t)$ is the observable and $G(s)$ is the fundamental quantity] or one starts from the Hamiltonian Eq. (2.1), when the coupling $g(s)$ is the fundamental quantity. The work of Voth and collaborators^{15–18} gives a strong indication that these two approaches are equivalent, as in the case of the position-independent friction.

Once the function $g(s)$ is known, one can make the following modification to the molecular dynamics Kramers–Grote–Hynes scheme we outlined in the introduction.

(a) Fix the proton at some position s and run a MD simulation. The friction kernel is calculated from the force–force correlation function.

(b) The previous step is repeated for several values of s .

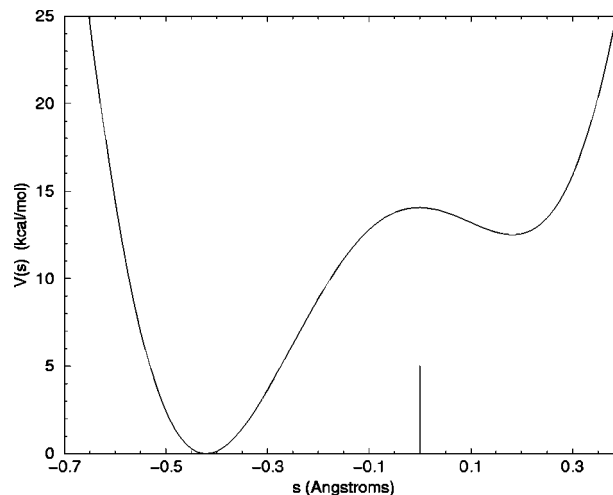


FIG. 1. The potential energy surface for the phenol-amine complex. The position of the transition state is shown at the bottom of the graph.

(c) The friction kernel $\gamma_s(t)$ is calculated and with the help of Eqs. (2.7)–(2.8); the coupling $g(s)$ is obtained. Then one solves for the Hamiltonian Eq. (2.1) to obtain the effective Grote–Hynes rate.

III. PROTON TRANSFER IN LIQUID METHYL CHLORIDE

As mentioned above, the system we will examine is the proton transfer reaction $AH-B \rightleftharpoons A^- - H^+ B$ in liquid methyl chloride, where the $AH-B$ complex corresponds to phenol-amine. There have been several recent quantum studies of this system. Azzouzz and Borgis²⁰ performed two calculations, one based on centroid theory and another on the Landau–Zener theory. The two methods gave similar results. Hammes-Schiffer and Tully²¹ used a mixed quantum-classical method and predicted a rate that is one order of magnitude larger, and a kinetic isotope effect that is one order of magnitude smaller than the Azzouzz–Borgis results. In a previous work¹ we performed a quantum calculation using the evolution operator technique we have developed^{22,23} and found results that agreed qualitatively with those of Azzouzz and Borgis. In this section we will examine how our previous results are affected when we allow for a position-dependent friction.

The potential for the phenol-amine complex is shown in Fig. 1. The intermolecular and the complex-solvent potentials have a Lennard–Jones and a Coulomb component as described in detail in Refs. 1, 20, and 21. In Ref. 1 we performed a MD simulation with one complex molecule and 255 solvent molecules. The temperature was fixed at 247 K. From MD simulation we obtained the friction kernel $\gamma(t)$. Once $\gamma(t)$ is known, one can calculate the spectral density $J(\omega)$, defined as the cosine Fourier transform of $\gamma(t)$:

$$J(\omega) = \frac{\pi}{2} \sum_k \frac{c_k^2}{m_k \omega_k} \delta(\omega - \omega_k). \quad (3.1)$$

Once $J(\omega)$ is known, the dynamics of the Hamiltonian Eq. (1.3) has been completely determined and we solved it using the exponential resummation method.^{22,23} We should point

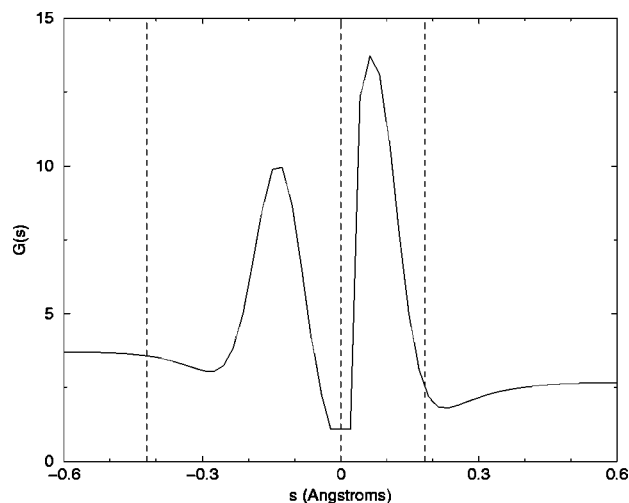


FIG. 2. $G(s)$ is the position-dependent part of the friction. It is not monotonic for reasons discussed in the text. The dashed lines denote the positions (from left to right) of the reactant well, the transition state, and the product well.

out that the dynamics of Eq. (1.3) depends on the bath parameters c_k, m_k, ω_k only in the combination that appears in Eq. (3.1); this statement just rephrases the fact that the dynamics of Eq. (1.3) is described by the generalized Langevin Eq. (1.1).

We found that the spectral density was peaked at low frequency (roughly 10 cm^{-1}), which means that most of the solvent modes are thermally excited. This is consistent with the assumption we have used that the spectral density of the bath can be approximated with the corresponding classical quantity. We also note that the decay time of the quantum flux-flux correlation function (which determines the time-scale of the quantum transfer process) was about 0.2–0.5 psec. This is much shorter than the characteristic timescale of the solvent (roughly 2π over the frequency at which the

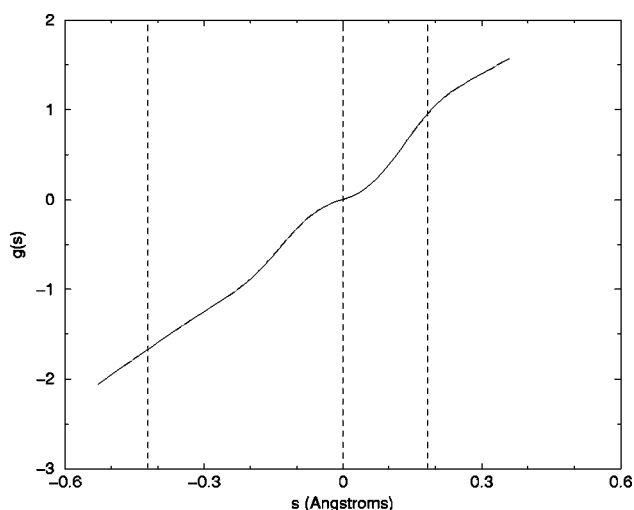


FIG. 3. The coupling function $g(s)$. The deviation from a straight line is the deviation from bilinear coupling. The positions of the transition state, the reactant, and product wells are also shown by the dashed vertical lines, similarly to Fig. 2.

TABLE I. Comparison of the ratio k/k_{ZPE} of the quantum rate k over k_{ZPE} , which is the TST result corrected for zero-point energy in the reactant well. Also shown are the Landau–Zener and centroid calculations from Ref. 20 and the molecular dynamics with quantum transition result from Ref. 21.

This work with full $g(s)$	This work with $g(s)=s$	Borgis (LZ)	Borgis (centroid)	Tully (MDQT)
9965	1150	907	1221	9080

spectral density is peaked), which is about 2.5–5 psec. In this sense, one can say that the proton is much “faster” than the “slow” solvent.

For the present work we modified our previous calculation as described in Sec. II: we fixed the proton at various positions and repeated the molecular dynamics simulation. We obtained the function $G(s)$, that we plot in Fig. 2, which is the position-dependent part of the friction kernel. We will postpone the interpretation of Fig. 2 until the end of this section. Using Eq. (2.8) we then calculated the coupling $g(s)$, which we show in Fig. 3. Once the coupling $g(s)$ is known, the Hamiltonian Eq. (2.1) has been fully determined and we can proceed with the calculation of the reaction rate. Similarly to our previous works on the quantum Kramers problem, we calculated the quantum reaction rate using the Miller–Schwartz–Tromp formula²⁴

$$k = \frac{1}{Q_R} \int_0^{+\infty} dt' C_f(t'), \quad (3.2)$$

where Q_R is the partition function of the reactants and $C_f(t)$ is the flux–flux correlation function

$$C_f(t) = \frac{1}{4m_s^2} \int d\mathbf{q} \int d\mathbf{q}' \times \left[\frac{\partial^2}{\partial s \partial s'} |\langle s' \mathbf{q}' | e^{-iHt_c} | s \mathbf{q} \rangle|^2 \right]_{s=s'=0}, \quad (3.3)$$

where m_s is the proton mass, $t_c = t - i\beta/2$ is the complex time, \mathbf{q} is a multidimensional bath coordinate and H is the quantum Hamiltonian Eq. (2.1). The integral is evaluated at the transition state $s = s' = 0$.

Our results for the quantum rate are presented in Table I. For comparison, we also show the results of Refs. 20, 21. The column $g(s)=s$ refers to the position-independent case, as calculated in our earlier work¹ on this system. Compared to our earlier results which assumed position-independent friction, the rate increased by an order of magnitude.

The calculated value for the H/D kinetic isotope effect (KIE) is shown in Table II. In order to understand this result we return to the Hamiltonian Eq. (2.1). The s -dependent part is

TABLE II. Comparison of the H/D kinetic isotope effects. The methods of calculation are the same as in Table I.

This work with full $g(s)$	This work with $g(s)=s$	Borgis (LZ)	Borgis (centroid)	Tully (MDQT)
37	83	40	46	3.9

$$V(s) + \sum_k \frac{c_k^2 g^2(s)}{2m_k \omega_k^2} + \mathbf{q}_0 \sum_k c_k g(s). \quad (3.4)$$

For this argument we consider the potential with the \mathbf{q} coordinates fixed at \mathbf{q}_0 because of the separation of timescales of the reaction coordinate transfer and solvent modes that was explained earlier. In Fig. 3 we can see that near the transition state, $s=0$, the function $g(s)$ is almost linear, which means that the third term in Eq. (3.4) is linear in s and the second is positive and proportional to s^2 . The square of the effective frequency at the top of the barrier is proportional to the second derivative of Eq. (3.4) with respect to s , which means that the frequency at the top of the barrier is reduced. Compared to the bilinear case this frequency reduction is larger, since the slope of $g(s)$ near the transition state $s=0$ is larger than the slope of the bilinear function $g(s)=s$. This “flattening” of the barrier top is responsible for the reduction of the value of the KIE.

We shall now discuss the shape of $G(s)$ that is shown in Fig. 2; in particular we have to explain why $G(s)$ is not a monotonic function, but has a maximum between the reactant well and the transition state. Let us recall a model nonlinear coupling function that has been used frequently in the literature:^{15,16,18}

$$g(s) = s + \epsilon s [1 - e^{-s^2/2\delta^2}], \quad (3.5)$$

where ϵ is a nonlinearity parameter, while the width parameter δ determines the length scale of the nonlinear coupling. For small displacements from the transition state $s \neq 0$, we can make a Taylor expansion of $g(s)$ and then calculate $G(s) \equiv (dg/ds)^2$:

$$G(s) \approx 1 + \frac{3\epsilon}{\delta^2} s^2 + \frac{9\epsilon^2 - 5\epsilon}{4\delta^4} s^4. \quad (3.6)$$

A very interesting feature of Eq. (3.6) is that there is a qualitative change as we move from strong to weak nonlinearity. For $\epsilon > 5/9$, Eq. (3.6) increases monotonically when we move away from the transition state. For weak nonlinearity however, when $\epsilon < 5/9$, $G(s)$ has the form of an inverted double well, exactly like our result in Fig. 2. Even though this argument explains the shape of $G(s)$ shown in Fig. 2, it is not very meaningful to carry this analogy further since the model function Eq. (3.5) assumes a symmetric potential energy surface. With this caveat in mind, in the framework of Eq. (3.5) the heights of the peaks of the function $G(s)$ shown in Fig. 2 correspond to a value of the nonlinearity parameter $\epsilon = 0.5$. This is smaller than the threshold value $5/9$ required for $G(s)$ to be nonmonotonic.

From Fig. 3 we note that $g(s)$ is almost linear (but with different slopes) in three regimes: the transition state, the bottom of the reactant well and the bottom of the product well. In other words, the $g(s)$ shown in Fig. 3 suggests that the coupling of the reaction coordinate to the bath is roughly bilinear, but with different coupling constants c_k in the three regions mentioned above. This situation bears remarkable resemblance to some early work by Robinson and coworkers²⁵ who had constructed a phenomenological model with two piecewise continuous GLEs, but with different friction kernels for the reactant and transition state regimes.

IV. DISCUSSION

In this paper we calculated the rate for a proton transfer reaction in liquid methyl chloride. In our previous work on this system we used a quantum Hamiltonian like Eq. (1.3) with bilinear coupling of the reaction coordinate to the bath. For the corresponding classical system, this approximation is equivalent to assuming that the dynamics is described by the GLE Eq. (1.1) with spatially independent friction. In that work we found results (second column in Tables I and II) that were in qualitative agreement with Ref. 20.

Numerical simulations have shown, however, that for some systems the friction kernel depends on the reaction coordinate. The GLE can be generalized for a spatially-dependent friction kernel as described in Eqs. (2.1)–(2.4). We performed a MD simulation that generated the coupling function $g(s)$ and our new quantum rate calculation resulted in a value nine times larger than our previous result that had assumed a position-independent friction. As can be seen in Table I, our result for the rate is now in very good agreement with Ref. 21. On the other hand, even though our new calculation for the H/D KIE reduced our previous result by more than half, it is still in better agreement with Ref. 20. Unfortunately, our calculation did not resolve the discrepancy between the results of Refs. 20, 21. Nevertheless, our work makes clear that relaxing the assumption of a spatially independent friction can have substantial effects on the calculated quantum reaction rate.

Only 10 years ago, a multidimensional quantum calculation of reaction rates in a condensed phase would be considered all but impossible and one would have to settle for some type of Landau–Zener calculation, or to use the Wolynes’ formula.²⁶ In the last 5 years such multidimensional quantum calculations have become routine after the development of several methods that we mention briefly below.

Our exponential resummation method,^{22,23} a Monte Carlo path integral method,²⁷ and Pollak’s perturbation method²⁸ all start from the Zwanzig Hamiltonian Eq. (1.3). The importance of spatially dependent friction points out the need for more microscopic quantum methods for multidimensional systems.

ACKNOWLEDGMENTS

The authors gratefully acknowledge the support of the chemistry division of the National Science Foundation through Grant No. CHE-9707858. We also acknowledge support of the Office of Naval Research and the NIH.

¹D. Antoniou and S. D. Schwartz, J. Chem. Phys. **110**, 465 (1999).

²D. Forster, *Hydrodynamic Fluctuations, Broken Symmetry, and Correlation Functions* (Addison-Wesley, Reading, MA, 1975).

³J. T. Hynes, in *The Theory of Chemical Reaction Dynamics*, edited by M. Baer (CRC, Boca Raton, FL, 1985), Vol. IV, p. 171.

⁴W. Keirsted, K. R. Wilson, and J. T. Hynes, J. Chem. Phys. **95**, 5256 (1991); B. J. Gertner, K. R. Wilson, and J. T. Hynes, *ibid.* **90**, 3537 (1989), and references cited therein.

⁵J. E. Straub, M. Borkovec, and B. J. Berne, J. Phys. Chem. **91**, 4995 (1987); J. Chem. Phys. **89**, 4833 (1988); J. E. Straub, B. J. Berne, and B. Roux, *ibid.* **93**, 6804 (1990).

⁶P. Hänggi, P. Talkner, and M. Borkovec, Rev. Mod. Phys. **62**, 251 (1991).

⁷H. A. Kramers, Physica (Utrecht) **4**, 284 (1940).

⁸R. F. Grote and J. T. Hynes, J. Chem. Phys. **73**, 2715 (1980); **74**, 4465

- (1981); P. Hänggi and F. Mojtabai, *Phys. Rev. A* **26**, 1168 (1982).
- ⁹R. Zwanzig, *J. Stat. Phys.* **9**, 215 (1973).
- ¹⁰E. Pollak, *Chem. Phys. Lett.* **127**, 178 (1986).
- ¹¹J. Onuchic and P. Wolynes, *J. Phys. Chem.* **92**, 6495 (1988).
- ¹²J. S. Bader, R. A. Kuharski, and D. Chandler, *J. Chem. Phys.* **93**, 230 (1990); N. Makri, E. Sim, D. E. Makarov, and M. Topaler, *Proc. Natl. Acad. Sci. USA* **93**, 3926 (1996).
- ¹³B. Carmeli and A. Nitzan, *Chem. Phys. Lett.* **102**, 517 (1983).
- ¹⁴E. Cortes, B. West, and K. Lindenberg, *J. Chem. Phys.* **82**, 2708 (1985).
- ¹⁵J. Strauss, J. Gomez-Llorrente, and G. Voth, *J. Chem. Phys.* **98**, 4082 (1993).
- ¹⁶G. Haynes and G. Voth, *J. Chem. Phys.* **103**, 10176 (1995).
- ¹⁷G. Voth, *J. Chem. Phys.* **97**, 5908 (1992).
- ¹⁸G. Haynes, G. Voth, and E. Pollak, *J. Chem. Phys.* **101**, 7811 (1994).
- ¹⁹E. Neria and M. Karplus, *J. Chem. Phys.* **105**, 10812 (1996).
- ²⁰H. Azzouzz and D. Borgis, *J. Chem. Phys.* **98**, 7361 (1993).
- ²¹S. Hammes-Schiffer and J. C. Tully, *J. Chem. Phys.* **101**, 4657 (1994).
- ²²S. D. Schwartz, *J. Chem. Phys.* **105**, 6871 (1996).
- ²³S. D. Schwartz, *J. Chem. Phys.* **107**, 2424 (1997).
- ²⁴W. H. Miller, S. D. Schwartz, and J. W. Tromp, *J. Chem. Phys.* **79**, 4889 (1983).
- ²⁵R. Krishnan, S. Singh, and G. Robinson, *Phys. Rev. A* **45**, 5408 (1992); *J. Chem. Phys.* **97**, 5516 (1992).
- ²⁶P. Wolynes, *Phys. Rev. Lett.* **47**, 968 (1981).
- ²⁷M. Topaler and N. Makri, *J. Chem. Phys.* **101**, 7500 (1994).
- ²⁸Y. Georgievskii and E. Pollak, *J. Chem. Phys.* **103**, 8910 (1995).